Reaction-to-Fire Testing and Modeling for Wood Products

Mark A. Dietenberger, Research General Engineer
Robert H. White, Supervisory Research Wood Scientist
Wood Preservation and Fire Research
USDA, Forest Service, Forest Products Laboratory
Madison, WI

ABSTRACT

In this review we primarily discuss our use of the oxygen consumption calorimeter (ASTM E1354 for cone calorimeter and ISO9705 for room/corner tests) and fire growth modeling to evaluate treated wood products. With recent development towards performance-based building codes, new methodology requires engineering calculations of various fire growth scenarios. The initial fire growth scenarios considered are those observed in 25-foot tunnel tests (ASTM E84) and room/corner tests to ensure continuity with existing building codes. We conducted specialized tests with the cone calorimeter to resolve fundamental inadequacies in modeling fire growth in wood products. These are noted as (1) effect of backing material on mass, heat, and smoke release rates and (2) effect of radiant flux on surface ignition, heat release rates, and smoke production rate. We demonstrated with analytical predictions of flame spread the complexities involved in modeling the initial fire growth scenarios, particularly for untreated and treated wood products. Despite these problems, it was possible to provide treatment guidelines in the form of desired time to ignition, peak heat release rate (HRR), and total heat release (THR) in cone calorimeter tests that will result in improved fire performance in the E84 or room/corner testing.

PREVIOUS RESEARCH ON FIRE RETARDANT WOOD WITH STANDARD FIRE TESTING

The Forest Products Laboratory (FPL) was an early innovator in development of fire-retardant treatments (FRTs) and their evaluation with bench-scale test methods. Many researchers still reference an early FPL report by Browne (1958), who provided a historical basis and the status of FRT technology for cellulose products. Various

works by FPL researchers are included in a major review by LeVan (1984) and a major reference book on fire retardants by Lyons (1970). With the advent of the plastics industry and because of the high flammability of plastics without treatment, research in flame retardancy of polymeric materials (of which wood became a subclass) was greatly advanced in the industry (Kuryla and Papa, 1978). By this time FRT of wood had become established as now represented in the AWPA Standard C20-99 (AWPA, 2000). At the 3rd BCC conference, White and Sweet (1992) discussed FPL research on FRT of wood. They addressed degradation of FRT plywood at elevated temperature and moisture levels, fire-resistive coatings for structural wood, and a combined preservative and retardant treatment for exterior applications. More recent work concerns a "holistic" approach to treating a wood composite for fire and decay (Lee and others, 1998; Chen, 1999).

A recent text on fire retardancy of polymeric materials edited by Grand and Wilkie (2000) describes a dramatic change in emphasis in test methods to evaluating treated materials with HRR calorimetry. One argument is that small tests (such as the limiting oxygen index test used mostly for plastics and the fire tube test used mostly for wood) have very poor correlation with full-scale fire performance but would still be suitable as quality control methods or screenings for newly developed materials. Indeed, some FRTs being examined at FPL for composite wood materials (including plastic components) have the problem of not showing fire retardancy on the basis of mass loss but are known to result in lowered heat of combustion or delay in time to ignition. In this case, the thermal gravimetric analysis (TGA) test and the fire tube test are useless. In the fire-retardancy text (Grand and Wilkie, 2000), the argument was even made that because the 25-foot Steiner tunnel does not properly rank plastics that melt and drip, and with its width being only 1.5 feet, it should be categorized as a smaller scale test useful for wood-based products. On the basis of the analytical flame spread model developed for the room/corner test (Dietenberger and Grexa, 1999) and for the Steiner tunnel, we show in this paper that the Steiner tunnel should still be thought of as a full-scale test, whereas the room/corner test has inherent design features that limit its range of application. Other limitations to the room/corner test were discussed in our earlier publication (White and others, 1999).

Some recent publications discuss the effect of FRT in wood as tested with the cone calorimeter. At the 10th BCC Flame Retardancy Conference, Wesolek and Kozlowski (1999) showed the effect of salt flame retardants and transparent intumescent systems on combustibility parameters measured in the cone calorimeter at fluxes of 35 and 50 kW/m^2. We have confirmed similar effects with the cone calorimeter. That is, the effective salt flame retardants reduced mass loss rate (MLR), effective heat of combustion (EHC), peak HRR, THR, and smoke extinction area (SEA), while increasing time to ignition (TTI) (Grexa and others, 2000; unpublished tests at FPL available on CD). Our unpublished tests of oriented strandboard (OSB) coated with a clear intumescent in 1997, or also coated with stucco in 1998, confirmed the effect is to decrease peak HRR somewhat, significantly increase TTI, and other parameters, MLR, EHC, THR, and SEA remained relatively unchanged. A more recent publication

by Kristoffersen and others (2001) is noteworthy in that whereas the effects of salt flame-retardants are confirmed, they also found that FRT concentration of 16% by weight is the most that is needed. FPL researchers also obtained this optimization of FRT using the fire tube test and Schlyter panel test nearly four decades ago (Eickner and Schaffer, 1967).

The cone calorimeter is not without its set of design limitations, but some particularly troublesome for wood-based materials need to be taken into account when correlating to large-scale tests. The first significant problem is the choice of an appropriate irradiant flux in which to use the combustibility properties, also discussed by Babrauskas in the fire retardancy text (Grand and Wilkie, 2000). After a review of various data for the room/corner test, Dietenberger and Grexa (1999) determined that the propane burner imposed a flux of approximately 55 kW/m^2 at the peak temperature position on the vertical sample. Results from Gandhi and others (1997) for the 25-foot Steiner tunnel showed that imposed flux is 49 kW/m^2 at the peak temperature position of 1 m from the methane burner position. Choosing an irradiance of 50 kW/m^2 in the cone calorimeter, one might obtain a time to ignition value that corresponds approximately to the full-scale tests. However, the flame existing on the cone calorimeter sample after piloted ignition imposes a flux of 12 kW/m^2 or more (which includes the adjustment for the surface burning temperature and the cone heater view factor). This means that the cone heater flux should be set at 12 kW/m^2 lower than the heat flux expected in a full-scale test (down to about 35 kW/m^2) to obtain a likely HRR profile of the exposed material for use in fire growth modeling or correlation.

Additional difficulties of the HRR profile indicated by Dietenberger and Grexa (1999) and shown in Dietenberger (1999) are as follows. The heavy thin backing board used in the 25-foot Steiner tunnel test often provides a heat sink sufficient to remove the second peak HRR commonly observed for wood products with insulation backing. In the specific case of OSB exposed to 50 kW/m^2, Figure 1 shows the dramatic elimination of the second peak HRR with the backing board behind the untreated sample, whereas Figure 2 for coated OSB and Figure 3 for FRT/coated OSB show significant reduction of second peak HRR with the backing board. Because of the time constant of 9 s for the gas analyzers, the "smoothed" HRR profile would need to be deconvolved to obtain a true HRR profile of the material. Not only that, one should also remove the HRR due to glowing combustion because the burner's flames in full-scale tests prevents oxidation of the char surface. One is left with a "corrected" HRR profile that approximates an exponential decay function, with somewhat increased peak HRR and a lowered flaming THR compared with the original measured HRR profile. One might even suggest that the original HRR profile obtained at 50 kW/m^2 approximates the "corrected" HRR profile corresponding to 35 kW/m^2, thus avoiding the corrections to the HRR profile needed for fire growth modeling. The presence of FRT in wood or intumescent coating on wood leads to a reduction in the first peak HRR as seen in Figures 1 to 3. In extreme cases, one should treat the "modeled" HRR profile as relatively flat during the test duration (this can be achieved by artificially

setting the flaming THR to very large values for use in the exponentially decaying HRR profile).

On the other hand, the first peak HRR for some wood products is very sharp (one example is redwood lumber), which presents a rather severe problem in obtaining reliable values with the cone calorimeter. That is, cone calorimeters with somewhat different time constants for the gas analyzers or with different time steps for data acquisition will be found to disagree sharply on the measured value of peak HRR. A numerical deconvolution of the HRR profile is not helpful either, because it usually results in unacceptable noise level in the derived true HRR profile. Another source of error in the peak HRR is that the initial wood volatiles can fail to be ignited with a spark, as can easily be seen in Figure 3. Contrast this to the expected complete combustion of the initial wood volatiles in the propane or methane burner environment in full-scale tests. These factors may lead some to abandon the use of peak HRR data as part of flammability assessment and instead use 5- or 10-min averaged HRR. However, our material database also includes a type X gypsum board and an FRT rigid polyurethane foam that have short burning times such that 5- or 10-min averaged HRR data would not fairly evaluate these materials.

Therefore, one must make the best possible use of the ignition conditions. This makes a flux of 50 kW/m^2 a better choice than 35 kW/m^2, because the time to ignition is not too fast for manual observation, while the combustible volatiles are relatively easy to ignite with the spark plug, particularly for many FRT wood materials. A data acquisition time interval of 1 s was found sufficient to effectively capture peak HRR. The time constants of gas analyzers were measured around 9 s and utilized in an analytical model of HRR profile by convoluting the gas analysis system response with an exponentially decaying "true" HRR profile. This analytical convolution function was fitted to HRR profile data to estimate true peak HRR (Dietenberger and Grexa, 1999). For OSB with various treatments, this function fitting is shown in Figures 1 to 3. Ultimately, one may occasionally have to resort to mechanistic modeling of wood pyrolysis (see Dietenberger, 2001) to obtain the correct HRR profile for use in numerical modeling of fire growth, particularly if fire retardants are involved.

The advantage of modeling materials with an exponentially decaying HRR profile during the duration of a fire test (typically 600 s or less) is that analytical prediction of flame spread is possible in some fire growth scenarios that include material burnouts. Such a model for flame spread in full-scale room/corner tests (Dietenberger and Grexa, 1999) had several features that were unavailable in early analytical fire growth models. The early models used the idea that flame propagation rate (rate of change in pyrolysis area) is proportional to the total HRR (in kW rather than in kW/m^2) and inversely proportional to TTI. The total HRR was in turn the sum of the burner output and the material HRR over the pyrolysis area. By assuming no sudden or gradual material burnout, one could show by analytic integration that the acceleration parameter of flame spread (as well as pyrolysis area and heat release rate) is controlled by the ratio of peak HRR over TTI. Brabrauskas (in Grand and Wilkie,

2000) used this ratio to show a linear correlation to the inverse of time to flashover in room/corner tests with the ceiling lined. A slight variation is to consider ratio of peak HRR over the time to the peak HRR, which is preferred in the European market (see Hees and Axelsson, 2001). However, this simple ratio was found to correlate poorly with the flame spread index (FSI) as defined in ASTM E84. Quintiere and Cleary (1991) included a sudden material burnout feature to their simple wind-aided flame spread analysis and derived the acceleration parameter in the flame spread solution to correlate with time to flashover in the database considered above by Babrauskas. Dillon and others (2001) provided a further modification by considering the exponentially decaying HRR profile. They used the corresponding exponential decay factor to replace the burnout time variable in the acceleration parameter to compare with time to flashover in the room/corner test as specified in NFPA 265 or NFPA 286. We applied these differing definitions of the acceleration parameter for predicting FSI and obtained poor results, particularly for gypsum board and FRT rigid polyurethane foam.

Results from our published analytic solution of flame spread in the room/corner test provide guidance to successfully correlate with both types of full-scale tests. The Steiner tunnel provides a simpler fire growth situation in that after ignition above the burner, the flames spread one-dimensionally in a relatively low-smoke ceiling layer through the tunnel. Whereas in the room/corner test, there are four phases of fire growth, namely, ignition, upward flame spread, three-dimensional lateral spread along the ceiling/upper wall, and downward flame spread near the flashover time. That the final phase, downward flame spread on the three walls, was successfully modeled as induced by thermal radiation from the hot smoky ceiling layer indicates the important factor of smoke concentration for room flashovers. Because one focus in this paper is to correlate combustibility parameters to full-scale performance, particularly FSI and time to flashover (TFO), by using the acceleration parameter, we simplify analytic solutions for HRR (in kW), flame areas, and pyrolysis areas as functions of time (Dietenberger and Grexa, 1999). The end result will be to realize Petrella's (1994) dream of organizing combustibility parameters of the cone calorimeter to guide flame retardancy.

ANALYTICAL MODEL OF INITIAL FLAME SPREAD FROM THE BURNER IN FULL-SCALE TESTS

What follows is the simplified version of the analytical room/corner flame spread model that does not include (1) multiple stages of fire growth resulting in restarts of the solution, (2) stepping up or down of the burner output, and (3) effect of time responses due to gas mixing in the upper gas layer or delayed gas analyzer sensing. Despite these simplifications, the fire growth acceleration parameters remain unchanged. The quasi-steady rate of flame spread (continuous movement of material heated to ignition as subjected to a moving but exponentially decaying flame heat flux profile) is represented as the rate of change of pyrolysis area as in the equation,

$$\dot{A}_{\mathrm{p}} = \frac{w\delta_{\mathrm{f}}}{\tau_{\mathrm{m}}} \approx \frac{a + bA_{\mathrm{p}} + c\dot{Q}_t}{\tau_{\mathrm{m}}} \qquad (1)$$

The total HRR from both burner and material (with exponentially decaying material HRR profile as function of time after initial ignition and of initial ignited area) is given by

$$\dot{Q}_t = \dot{Q}_{\mathrm{b}} + \dot{Q}''_{\mathrm{m,ig}} A_{\mathrm{ig}} \exp(-\omega_{\mathrm{m}} t) + \int_0^t \dot{Q}''_{\mathrm{m.ig}} \exp(-\omega_{\mathrm{m}}(t-\xi))\dot{A}_{\mathrm{p}}\, d\xi \qquad (2)$$

The materials in our database behave as thermally thick materials at fluxes of 50 kW/m^2, which means the formula for material time constant is proportional to the time to ignition as

$$\tau_{\mathrm{m}} = k\rho C_{\mathrm{p}} \left(\frac{T_{\mathrm{ig}} - T_{\mathrm{m}}}{\dot{q}''_{\mathrm{w}} - \dot{q}''_{\mathrm{ig}}} \right)^2 \approx (4/\pi)\mathrm{TTI} \qquad (3)$$

For materials that are thermally thin, the time constant is equal to TTI except when the backing board commonly used for full-scale test affects the thermal response time. The material HRR decay parameter is related to the THR of a completely charred, 12.5-mm-thick sample by the equation

$$\dot{Q}''_{\mathrm{m,ig}} / \omega_{\mathrm{m}} = \int_0^\infty \dot{Q}''_{\mathrm{m,ig}} \exp(-\omega_{\mathrm{m}} t) dt \approx (12.5/\delta_{\mathrm{m}}) \int_0^\infty \dot{Q}''_{\mathrm{m,cone}}\, dt = \mathrm{THR}(12.5/\delta_{\mathrm{m}}) \qquad (4)$$

We note the THRs used in the functional fits to the HRR profiles in Figures 1 to 3 are the measured values for OSB samples, which are typically 12.5 mm thick. The Laplace transform of Equation (1) into the frequency domain, s, is,

$$s\tilde{A}_{\mathrm{p}} - A_{\mathrm{ig}} = \frac{a + c\dot{Q}_{\mathrm{b}}}{s\tau_{\mathrm{m}}} + \frac{b\tilde{A}_{\mathrm{p}}}{\tau_{\mathrm{m}}} + \frac{c\dot{Q}''_{\mathrm{m.ig}} A_{\mathrm{ig}} + c(s\tilde{A}_{\mathrm{p}} - A_{\mathrm{ig}})\dot{Q}''_{\mathrm{m,ig}}}{(s+\omega_{\mathrm{m}})\tau_{\mathrm{m}}} \qquad (5)$$

Rearrangement of Equation (5) to solve for the pyrolysis area in frequency domain is given by

$$\tilde{A}_{\mathrm{p}} = \frac{(s+\omega_{\mathrm{m}})\left(A_{\mathrm{ig}} + \dfrac{a + c\dot{Q}_{\mathrm{b}}}{s\tau_{\mathrm{m}}} \right)}{\left((s - b/\tau_{\mathrm{m}})(s+\omega_{\mathrm{m}}) - \dfrac{cs\dot{Q}''_{\mathrm{m,ig}}}{\tau_{\mathrm{m}}} \right)} \qquad (6)$$

Zero for the denominator of Equation (6) result in two roots,

$$s_i = \frac{b + c\dot{Q}''_{\mathrm{m.ig}} - \omega_{\mathrm{m}}\tau_{\mathrm{m}}}{2\tau_{\mathrm{m}}} - (-1)^i \sqrt{\left(\frac{b + c\dot{Q}''_{\mathrm{m,ig}} - \omega_{\mathrm{m}}\tau_{\mathrm{m}}}{2\tau_{\mathrm{m}}} \right)^2 - \frac{b\omega_{\mathrm{m}}}{\tau_{\mathrm{m}}}} \qquad (7)$$

It is often asserted that if the roots are positive, then the fire growth is accelerative while negative values for the roots the fire is dying out despite flame spreading. If the square root integrand is also negative, the fire growth has an oscillation behavior or at least has a peak RHR. The solution for the pyrolysis area is the Laplace inverse transform of Equation (6), and the total heat release can be obtained by applying Equation (2). The result for time after ignition, t, is,

$$A_p = \left(\frac{a + c\dot{Q}_b}{\tau_m} + A_{ig}\omega_m \right) \left(\frac{\exp(s_1 t) - \exp(s_2 t)}{s_1 - s_2} \right) + \left(\frac{a + c\dot{Q}_b}{\tau_m} \right) \left(\frac{\omega_m}{s_1 - s_2} \right) \left(\frac{\exp(s_1 t) - 1}{s_1} - \frac{\exp(s_2 t) - 1}{s_2} \right) + A_{ig} \left(\frac{s_1 \exp(s_1 t) - s_2 \exp(s_2 t)}{s_1 - s_2} \right) \quad (8)$$

$$\dot{Q}_t = \dot{Q}_b + \frac{(a + c\dot{Q}_b)\dot{Q}''_{m,ig}}{\tau_m} \left(\frac{\exp(s_1 t) - \exp(s_2 t)}{s_1 - s_2} \right) + \dot{Q}''_{m,ig} A_{ig} \left(\frac{s_1 \exp(s_1 t) - s_2 \exp(s_2 t)}{s_1 - s_2} \right) \quad (9)$$

We note that Equation (8) allows the pyrolysis area to continue to increase with time even while Equation (9) provides for the total HRR to first increase and then decrease in value as function of time. This was clearly demonstrated for the room/corner tests (Dietenberger and Grexa, 1999). Early analytical flame spread models were not capable of this feature because a proportionality between the pyrolysis area and material HRR was assumed to hold in Equation (1), thereby resulting in simpler solutions in place of Equations (8) and (9).

Various terms in Equations (7) to (9) can be examined to note any similarities and differences between the Steiner tunnel and the room/corner tests. First, the material time constant given by Equation (3) would be similar between the two full-scale tests. That is, the material thermal inertia, ignition temperature, ambient temperature, imposed heat flux at point of ignition, and critical heat flux values are about the same between the two tests for the same material. We note that results in the literature and from our laboratory indicate that ignition temperature, critical flux, and material thermal inertia can be considered constant in a given test apparatus for the imposed heat fluxes, that is, at least 5 to 10 kW/m^2 greater than the critical heat flux values. We provide the example of TTI plotted versus irradiance for the three OSB samples in Figure 4. Because the materials in our database can be considered thermally thick for their typical time to ignition in the full-scale tests, the differences in the use of backing board in the full-scale tests will not affect the material time constant either. The total heat release (THR) as measured in the cone calorimeter varies little with imposed flux (but at least 5 to 10 kW/m^2 greater than the critical heat flux) or with the backing conditions (as long as the specimen is not so thick that the char front does not reach the back end of the specimen). Figure 5 provides such an example for the three OSB samples. Most materials were around 12.5 mm thick, so that one would not have a problem with incomplete charring of the specimen in the cone calorimeter. The combustibility parameter that Equations (8) and (9) have considerable sensitivity to is

peak HRR, which also can increase significantly with imposed heat flux, as shown for the three OSB samples in Figure 6. Combining this effect with the problems associated with measuring peak HRR in the cone calorimeter indicates that serious attention should be given to ensuring the reliability of the profile near the peak HRR. Because peak HRR occurs shortly after ignition for most wood products, including some with FRT, the peak HRR ought to be similar between the large-scale tests because their imposed heat flux at ignition are also about the same. The differences based on combustibility properties as measured in the cone calorimeter will probably be associated with the second peak HRR commonly observed with charring materials, because the imposed flux will have some unknown value as the test nears the end. The remaining terms are the coefficients $a, b, \& c$ and the initial ignited area, A_{ig}, which are the characteristics of a full-scale test and can be significantly different between the Steiner tunnel and the room/corner test. For the upward fire growth stage in the room/corner test, these coefficients were derived by Dietenberger and Grexa (1999), resulting in

$$\frac{A_f - A_p}{c_f} = a + bA_p + c\dot{Q}_t \approx \frac{A_{fu}}{5.6c_f} - \frac{A_p}{c_f} + \frac{0.0051\dot{Q}_t}{c_f} \quad (10)$$

$$c_f = (y_f - y_p)/\delta_f \approx 1.3 \quad (11)$$

Acceptable accuracy was obtained by setting the initial ignition area, A_{ig}, to zero in the model. In the case of the 25-foot Steiner tunnel, the data of Parker (1977) were correlated and resulted in

$$\frac{A_f - A_p}{c_f} = a + bA_p + c\dot{Q}_t \approx \frac{-2.83w}{c_f} - \frac{A_p}{c_f} + \frac{0.022\dot{Q}_t}{c_f} \quad (12)$$

Because the coefficient b is negative for both tests, the square root integrand in Equation (7) is positive, implying that the roots s_i are real numbers and making Equations (7) to (9) suitable for spreadsheet applications, whereas a specialized Fortran program was written for the more sophisticated room/corner flame spread model. The coefficient c in Equation (12) is 4.3 times larger than that in Equation (10) and accounts for the Steiner tunnel being a more severe test than the room/corner test. Indeed, various studies of flame spread in tunnels with assisting forced airflow have shown the slopes of the flame area as function of heat release rate to have values around 0.022 m²/kW. We then note the coefficients $b \& c$ are independent of scale and the coefficient a is proportional to the flame-width impinging on the test specimen for both Equations (10) and (12). This means that both the Steiner tunnel test and the room/corner test are suitable as full-scale flame spread tests. Furthermore, it appears that both tests are complementary, as we demonstrate in the next section on guidance for flame retardancy.

For evaluating the remaining coefficients for the Steiner tunnel, we tested samples of treated and untreated OSB (and Red Oak as well) in the cone calorimeter. (Flame-spread data and the samples were provided by James White of Western Fire Center, Inc.) The combustibility parameters are shown with Figure 7 for the imposed flux set at 50 kW/m². Equations (7) to (9) were programmed on the Sigma Plot spreadsheet

(SPSS, Inc.), and the fit to the data for all four materials resulted in the following coefficient values for the Steiner tunnel:

$$c_f \approx 11.7, \quad A_{ig} = 0, \quad \& \quad \tau_{burner} = 18 \text{ sec} \qquad (13)$$

We note that the burner has an imposed heat flux response function in which we estimate the time constant at 18 s. In the flame spread model for the room/corner test, we showed the effective time for material ignition in the large-scale test is the sum of the burner time constant and the time to ignition as measured in the cone calorimeter. In Figure 7, the model predicts the higher FSI materials quite well but seems to poorly predict the flame spread for OSB having both FRT and intumescent coating. However, the cone calorimeter's spark plug seems to have trouble igniting the considerable mass loss during the first minute of exposure. Indeed, examination of both mass loss rate and white smoke production rate indicate a similarity to the profile of the OSB with just the intumescent coating, which might suggest a similar, much reduced time to ignition if a more effective igniter is used. Figure 3 verifies the high error in the TTI and its effect on the HRR profile. A smaller value for TTI resulted in a better fit to the data shown as the dash line in Figure 7, which also show a steady flame spread propagation.

GUIDANCE ON FLAME RETARDANCY TO ATTAIN DESIRED FSI OR TFO

Further simplification can be achieved if our attention is focused on the neutral zone between the accelerative and damped fire growth. This occurs when the roots calculated from Equation (7) are relatively close to zero. Close examination of Equation (9) for the total HRR shows that for small values of the roots and at small times, the direction of fire growth is dominated by the sum of the roots and multiplied by the material time constant. Thus, the acceleration parameter is defined as

$$\beta = (s_1 + s_2)\tau_m = b + c\dot{Q}''_{m,ig} - \omega_m \tau_m \qquad (14)$$

The neutral point is the acceleration parameter at zero, or $\beta = 0$. Specifying the acceleration parameter to some positive value will indicate a degree of fire growth acceleration above that of a steady growth. Likewise, a negative value will give a degree of damping the fire growth after ignition. Substituting in the material HRR decay parameter from Equation (4) into Equation (14) and rearranging, we consider the simple and intriguing function,

$$\frac{Q''_{m,cone}}{\tau_m} = \left(c + \frac{b - \beta}{\dot{Q}''_{m,ig}} \right)^{-1} \qquad (15)$$

This function indicates that the ratio, $\text{THR}(12.5/\delta_m)/(4(\text{TTI})/\pi)$, should be on the vertical axis and the corresponding peak HRR should be on the horizontal axis. This is shown in Figures 8 and 9 for all our room burn materials tested in the cone calorimeter at 50 kW/m^2. The curves for the Steiner tunnel and room/corner tests from Equation (15) for various values of the acceleration parameter β are also shown in the two figures. We note that for the gypsum board, although its peak HRR is greater than that of materials with FRT, is unique among the materials in being positioned far below the

Steiner tunnel neutral curve. We also note that the remaining materials of Class A are slightly below the Steiner tunnel neutral curve, meaning that their flame spread process is at least damped. The materials considered as Class B or C are much further beyond the Steiner tunnel neutral curve but are still below the room/corner neutral curve. Thus, in the Steiner tunnel the Class C materials are very accelerative, while in the room/corner test they have an initial fire growth followed by a damping of HRR (and pyrolysis area continues to increase but at a reduced rate). The achievement of flashover in the room occurs by additional fire growth phenomena, the downward flame spread (or ceiling spread under highly combustible ceiling materials) motivated by the hot, smoky ceiling gas layer.

To more clearly show these various effects, the plot of FSI versus acceleration parameter of the Steiner tunnel is shown in Figure 10. Because the gypsum board has a very short burn time, and with the formula for computing FSI (see ASTM E84) overlooking this factor, its FSI is "artificially" higher than its real flame spread behavior. It is noted three different types of Class A materials (FRT plywood, FR polyurethane rigid foam, and coated/treated OSB) are relatively close together, with β slightly less than zero, and yet are much beyond the gypsum board data, which has $\beta \leq -3$. Finally, as the acceleration parameter is greater than 0.184, the FSI is beyond 75 and exhibits a high sensitivity to the combustibility parameters, which we attribute to the affects of tunnel size limitation to the calculation of FSI. One notes that the redwood seems to have a too high of an acceleration parameter due to its sharp peak HRR not being consistent with a decaying exponential profile. If, however, these problems with correlating to FSI become persistent and common enough, a numerical model of flame spread would be required to predict FSI.

In the case of the room/corner test, TFO versus acceleration parameter is shown in Figure 11 for the materials on walls only scenario and in Figure 12 for materials on walls and ceiling scenario. It seems that materials with high smoke development (FR polyurethane foam and pressboard) need a severe adjustment to the acceleration parameter (as shown in Figures 11 and 12) to account for the accelerating potential of high thermal radiation due to the heavy smoky ceiling layer. Our previous paper on smoke correlations (Dietenberger and Grexa, 2000) suggests using the peak SEA at cone heater fluxes higher than 30 kw/m^2 on horizontal samples for correlating with smoke production in the room/corner tests. So in the case of Figure 11, the acceleration parameter was adjusted by adding the term, peak SEA/3000, and in Figure 12, peak SEA/1500. The smoke effect seems to double when a ceiling material is involved. As a result, anomalous performance behavior of the FR polyurethane rigid foam in the three testing scenarios is explained.

For fire retardancy guidance we begin with Figures 8 and 9. If untreated materials are located high on the vertical scale (above 2,000 kW/m^2) and near the room/corner neutral curve like the wood materials, the retardancy strategy is to reduce the peak HRR to below 100 kW/m^2 to approach Class A treatment. This is easily done with the

salt fire retardants as shown in the Figure 13 for various FRT with 16% treatment by weight of southern yellow pine and hard maple. This treatment mainly works by significantly increasing the char content and decreasing the combustible tar portion of the wood volatiles. Smoke and carbon monoxide production were also reduced because of the reduction of the combustible tar in the wood volatiles (also see Dietenberger, 2001, for mechanistic kinetics of wood pyrolysis and their heat of combustion). However, there are exceptions, such as diammonium phosphate (DAP) and $ZnCl_2$, which increase specific smoke production (see also Eickner and Schaffer, 1967).

In the case of plastic-based materials, we replotted Petrella's data for wire and cable coatings according to our new procedure, with the result in Figure 14. The wide range of combustibility parameters is noted and demonstrates the cone calorimeter versatility. One finds five of the coating types that could be classified as Class A, one of the coating types as being similar to the coated OSB (Class B), and three coating types that would lead to quite easy flashover in the room/corner test. Indeed, it appears that KYNAR and GW-3000D (Petrella, 1994) have very low combustibility, like the gypsum board. One should not forget the adjustment needed to the acceleration parameter of the room/corner tests due to the high smoke production of certain thin panels and some plastic products.

SUMMARY AND CONCLUSION

In this paper we reaffirmed the 25-foot Steiner tunnel as a full-scale test method, particularly in its good sensitivity in sorting out the treated materials and very low combustible materials. The room/corner test is limited in that it is not as severe as the Steiner tunnel and may have some trouble sorting out treated materials. Even with the room burner set at 300 kW, the room/corner test still would not be as severe as the Steiner tunnel test. The versatility of the cone calorimeter was demonstrated, although one must be cautious in interpreting and using combustibility parameters, particularly that of TTI, peak HRR, and peak SEA. Because of concerns in the reliability of these parameters, we have begun experimentation using an auxiliary Bunsen ring burner in the effluent stream of the volatiles. This option should allow reduction in the cone heater flux (perhaps to 35 kW/m^2), eliminate the white smoke, ignite the wood volatiles more effectively, and develop the HRR profile more consistent with that of the full-scale tests. With this efficient combustion of the volatiles, it might even be possible to derive global mechanistic kinetic properties of wood pyrolysis (Dietenberger, 2001). In consideration of these problems, it was still possible to organize combustibility properties suitable for both wood and plastics and relative to performances in both the Steiner tunnel and the room/corner tests. Presentation of the fire performance data as in Figures 8 and 9 also lends itself to varying the fire retardancy of materials (particularly composites) to the amount needed to achieve a Class A or B from a formerly Class C or D material status. One does not have to adjust the neutral curve for the Steiner tunnel because of high smoke production, whereas the neutral curve for the room/corner test may need to be adjusted inward to

account for the accelerating effects of excessive smoke. Finally, the analytical fire growth model as presented for spreadsheet applications was used to obtain a physical understanding of fire growth processes at full-scale, indicate sensitivities to different combustibility parameters, and provide the theoretical basis as to the use of the acceleration parameter for classifying materials.

NOMENCLATURE

A Area, m^2 δ Feature dimension, m
$a, b, \& c$ Fire growth coefficients, Equation (1) ρ Material density, kg/m^3
$c_f = (y_f - y_c)/\delta_f$ τ Time constant, s
C_p Heat capacity, J/Kg ω Exponential time decay coefficient, 1/s
k Thermal conductivity, kW/Km *Subscript definitions*
$\dot{Q}$ Rate of heat release (RHR), kW b Propane ignition burner
$\dot{q}''$ Heat flux, kW/m^2 f Flames adjacent to material
s_i Singularities of transform, Equation (6) ig Ignition condition
T Temperature, K m Material property or condition
t time, s p Pyrolyzing condition
w Burner width, m w Wall of the room
y Surface distance, m

REFERENCES

AWPA, 2000, Structural Lumber-Fire Retardant Treatment by Pressure Processes, AWPA Standard C20-99, Granbury, TX.

Browne, F.L., 1958, Theories of the Combustion of Wood and Its Control, USDA Forest Service, Forest Products Laboratory, Report No. 2136.

Chen, G.C., 1999, Synthesis and Evaluation of Borates derived from Boric Acid for Fire and Decay Protections, In Lewin, M., Ed. Proceedings of 10th annual BCC conference on flame retardance; May 19-21, Stamford, CT. Norwalk, CT: Business Communications Company, Inc.; 1999: 365-380.

Dietenberger, M.A., 1999. Effect of Backing Board on the Heat Release Rate of Wood Products. Proceedings of International Conference on Fire Safety, Vol. 28; 1999 July 26-30, Columbus OH: Product Safety Corporation, Sissonville, W. Va., 62-73.

Dietenberger, M.A., 2001. Update for Combustion Properties of Wood Components. In: Fire and Materials 2001 7th International Conference; January 22-24, 2001; Fisherman's Wharf, San Francisco, USA. London: Interscience Communications Ltd., 159-171

Dietenberger, M.A. and Grexa, O., 1999, Analytical Model of Flame Spread in Full-scale Room/corner Tests (ISO9705). In: Fire and Materials 1999 6th International Conference; 1999 February 22-23; San Antonio, TX. London: Interscience Communications Ltd, 211-222.

Dietenberger, M.A. and Grexa, O., 2000. Correlation of Smoke Development in Room Tests With Cone Calorimeter Data for Wood Products. Proceedings of 4th International Scientific Conference on Wood & Fire Safety, 2000 May 14-19, The High Tatras, Hotel Patria, Strbske Pleso, Slovak Republic, 45-56

Dillon, S.E., Janssens, M.L., and Hirschler, M.M., 2001, Using the Cone Calorimeter as a Screening Tool for the NFPA 265 and NFPA 286 Room Test Procedures, In: Fire and Materials 2001 7th International Conference; January 22-24, 2001; Fisherman's Wharf, San Francisco, USA. London: Interscience Communications Ltd., 527-539.

Eickner, H.W. and Schaffer, E.L., Fire-retardant Effects of Individual Chemicals on Douglas Fir Plywood, Fire Technology journal, Vol.3, No. 2, May 1967, 90-104.

Gandhi, P.D., Caudill, L., Hoover, J. and Chapin, T., 1997, Determination of Fire Exposure Heat Flux in Cable Fire Tests, in: Hasemi, Y., Ed., Fire Safety Science – Proceedings of the Fifth Int. Sym., World Congress Centre, Melbourne, Australia, March 3-7, Int. Asc. for Fire Safety Science, 141-151.

Grand, A.F. and Wilke, C.A. (eds.), 2000, Fire Retardancy of Polymeric Materials, New York, Marcel Dekker, Inc.

Grexa, O., White, R.H., and Dietenberger, M.A., 2000, Flame Retardant Treated Wood Products. In: Osvald, I.A., Ed., Proceedings of 4th Int. Conf. on Wood & Fire Safety, The High Tatras, Slovak Republic, May 15-18, 2000, Published by Technical University of Zvolen, Slovak Republic, 101-110.

Hees, P.V. and Axelsson, 2001, Mathematical Modelling of Fire Development in Cable Installations, In: Fire and Materials 2001 7th International Conference; January 22-24, 2001; Fisherman's Wharf, San Francisco, USA. London: Interscience Communications Ltd., 23-37.

Kristoffersen, B., Hansen, A.S., and Hovde, P.J., 2001, Optimization of Fire Retardant Treated Wood, In: Fire and Materials 2001 7th International Conference; January 22-24, 2001; Fisherman's Wharf, San Francisco, USA. London: Interscience Communications Ltd., 173-184.

Kuryla, W.C. and Papa, A.J. (eds.), 1978, Flame Retardancy of Polymeric Materials, Vol. 4 , New York, Marcel Dekker, Inc.

Lee, H., Chen, G.C., and Rowell, R.M., 1998, Flame Retardant and Fungal Decay Resistant Properties of Wood Reacted with Phosphorus Pentoxide-Amines System, In Lewin, M., Ed. Proceedings of 9th annual BCC conference on flame retardance; May 19-21, Stamford, CT. Norwalk, CT: Business Communications Company, Inc.; 1998: 98-119.

LeVan, S.L., 1984, Chapter 14. Chemistry of Fire Retardancy. In Rowell, Roger M., The chemistry of solid wood, Advances in chemistry series 207. Washington, DC: ACS; 1984

Lyons, J.W., 1970, Chapter 4. Cellulose: Chemistry, Wood, Paper, and Forest Fire Control in The Chemistry and Uses of Fire Retardants , New York: John Wiley & Sons, Inc., 1970

Parker, W.J., 1977, An Investigation of the Fire Environment in the ASTM E 84 Tunnel Test, NBS-TN-945, NIST, Gaithersburg, MD.

Petrella, R.V., 1994, The Assessment of Full-Scale Fire Hazards from Cone Calorimeter Data, Journal of Fire Sciences, Vol. 12, Jan/Feb 1994, 14-43.

Quintiere, J. and Cleary, T., 1991, Simple Wind-Aided Flame Spread Model, NISTIR-91-4664, NIST, Gaithersburg, MD.

Wesolek, D. and Kozlowski, R., 1999. The Influence of Some Flame Retardants on the Flammability of Wood Studied by Cone Calorimeter. In: Lewin, M., Ed. Proceedings of 10th annual BCC conference on flame retardance , May 24-26, 1999, Stamford, CT. Norwalk, CT: Business Communications Company, Inc.

White, R.H. and Sweet, M.S., 1992, Flame Retardancy of Wood: Present Status, Recent Problems, and Future Fields, In Lewin, M., Ed. Proceedings of 3rd annual BCC conference on flame retardance; May 19-21, Stamford, CT. Norwalk, CT: Business Communications Company, Inc.; 1992: 250-257.

White, R.H., Dietenberger, M.A., Tran, H., Grexa, O., Richardson, L.,Sumathipala,K. and Janssens, M., 1999, Comparison of Test Protocols for the Standard Room/Corner Test, Fire and Materials journal, Vol.23, pp.139-146.

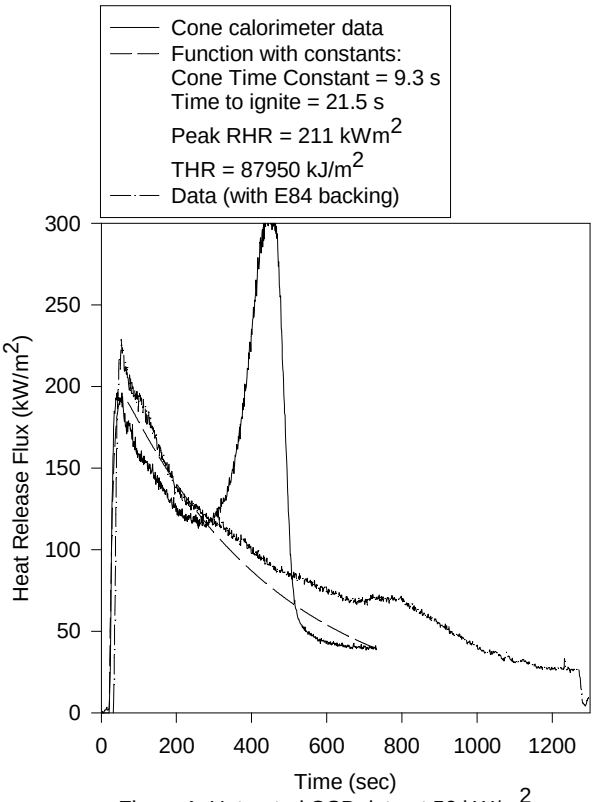

Figure 1. Untreated OSB data at 50 kW/m^2

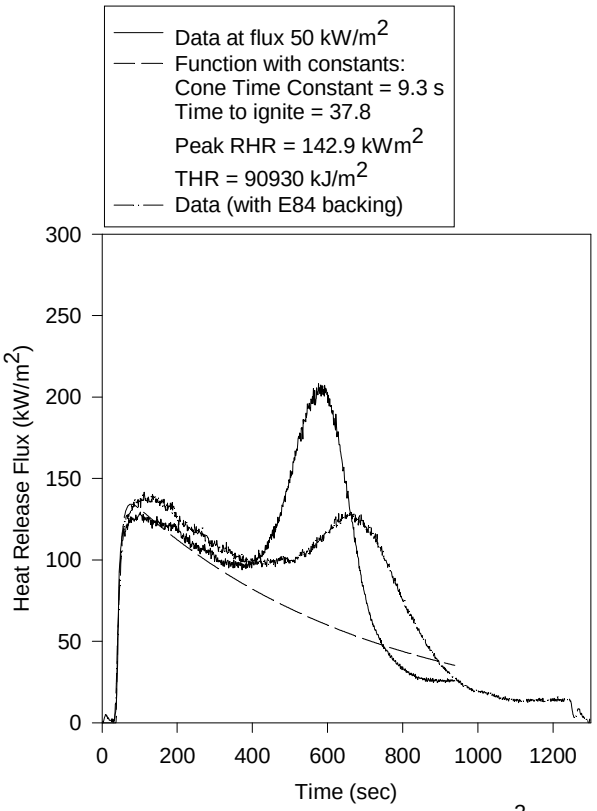

Figure 2. Coated OSB data at 50 kW/m^2

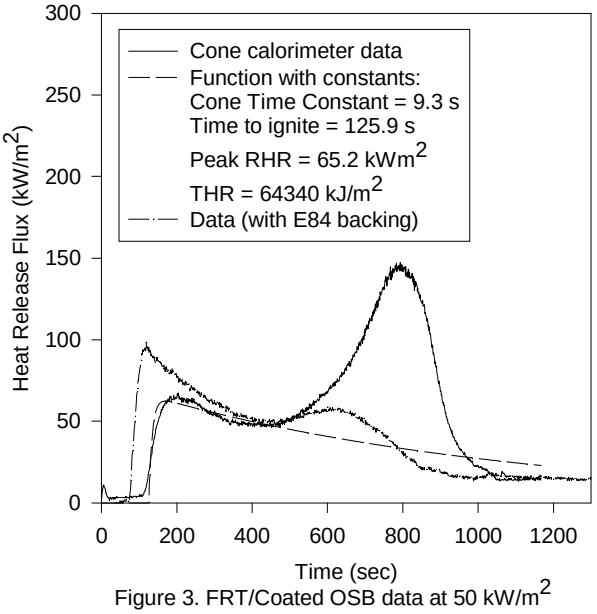

Figure 3. FRT/Coated OSB data at 50 kW/m^2

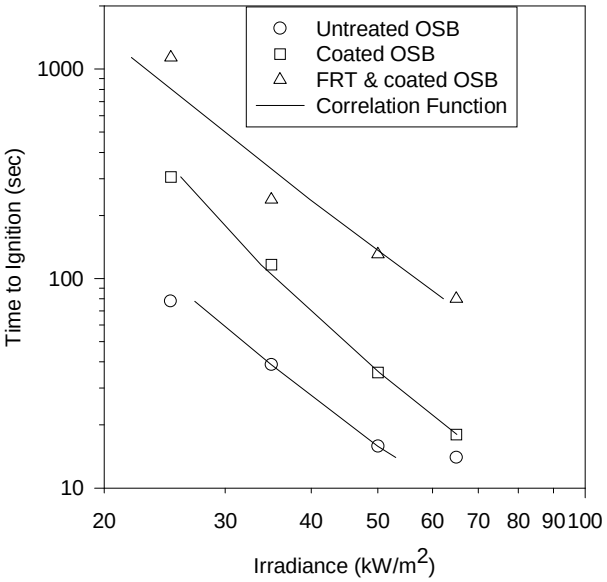

Figure 4. Correlation of time of ignition for OSB tested in Cone Calorimeter with various levels of FRT

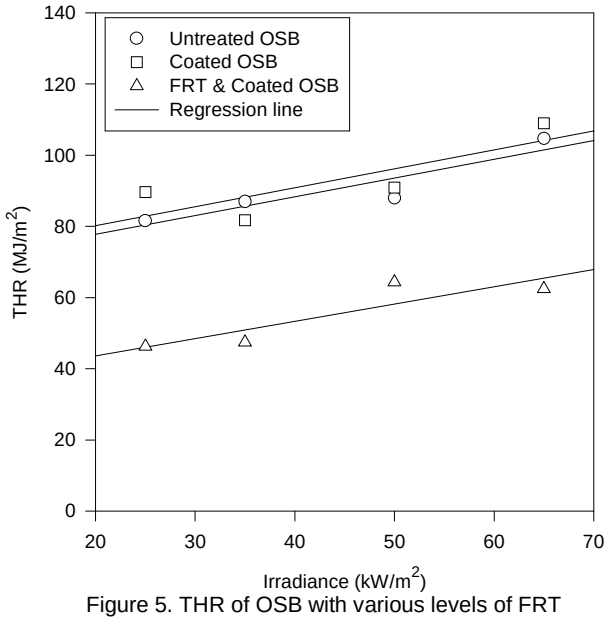

Figure 5. THR of OSB with various levels of FRT

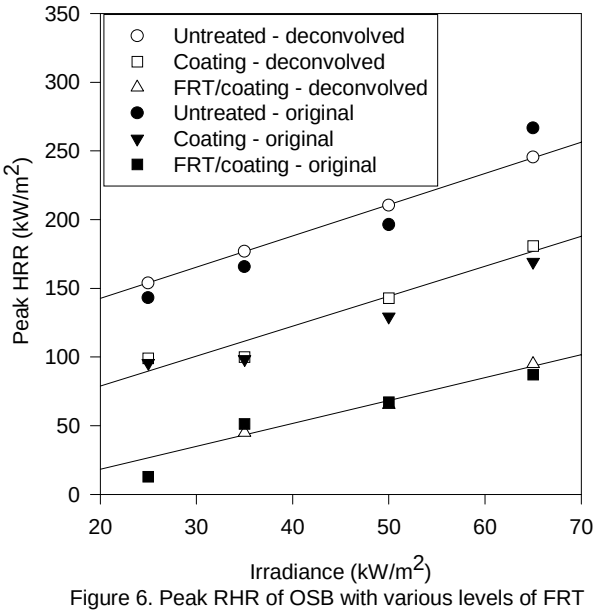

Figure 6. Peak RHR of OSB with various levels of FRT

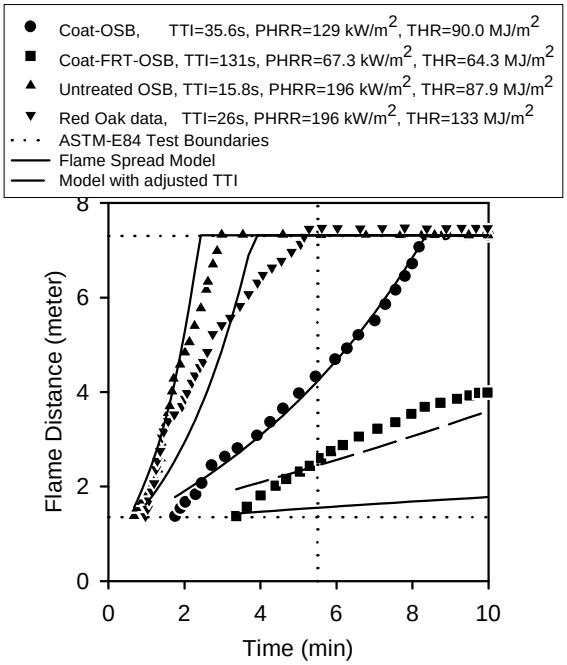

Figure 7. Prediction of Flame Spread Distance

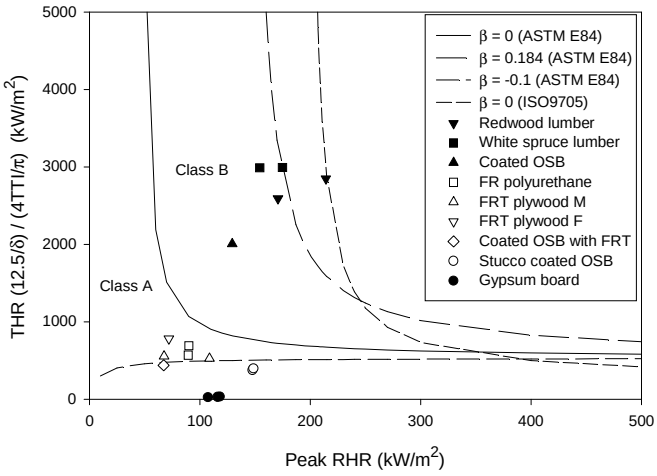

Figure 8. Initial fire growth propensity of Class A and B materials

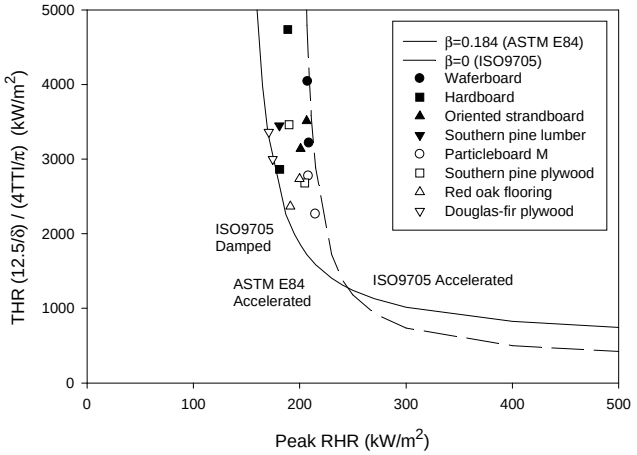

Figure 9. Initial fire growth propensity of Class C materials

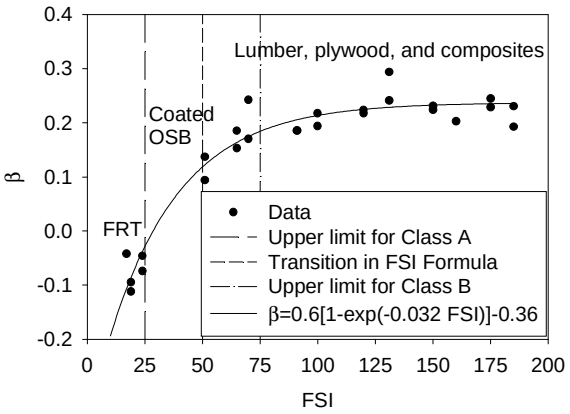

Figure 10. β as function of Flame Spread Index

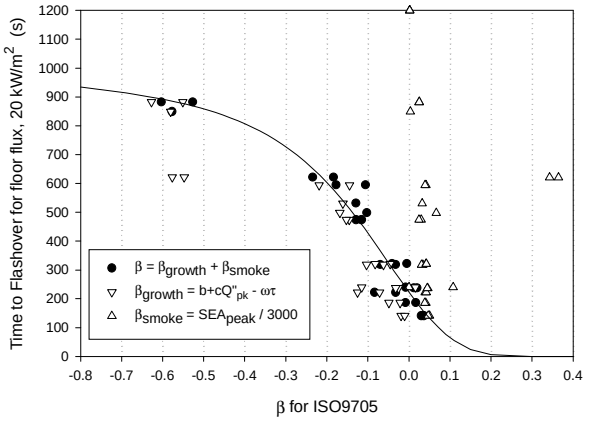

Figure 11. Time to Flashover Correlation - Wall only data

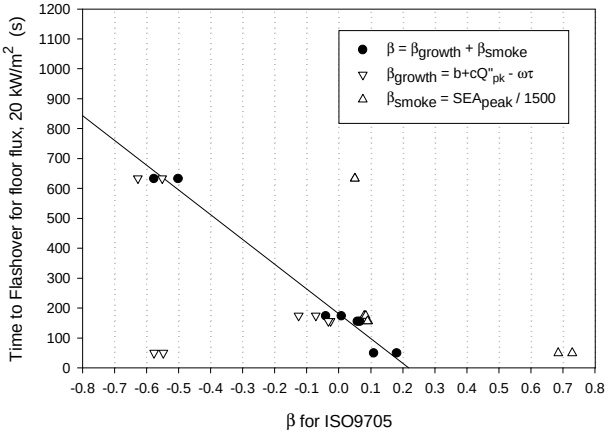

Figure 12. Time to Flashover Correlation - wall and ceiling

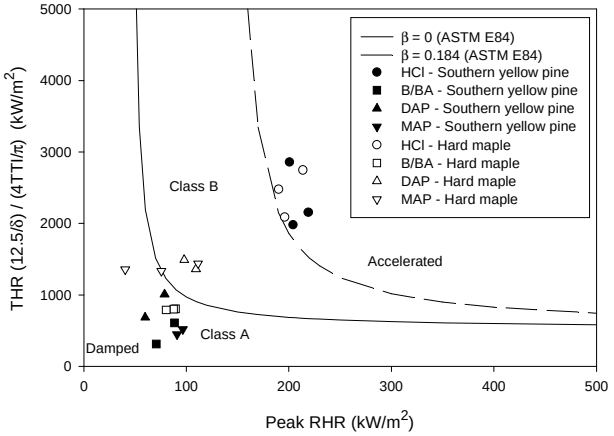

Figure 13. Initial Fire Growth Propensity with Various FRT wood

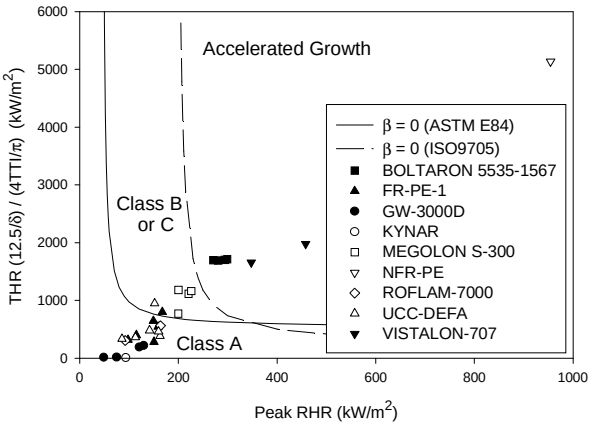

Figure 14. Initial fire growth propensity of wire and cable coatings

Dietenberger, Mark A., White, Robert H. Reaction-to-fire testing and modeling for wood products. IN: Twelfth Annual BCC Conference on Flame Retardancy, May 21-23, 2001, Stamford, CT. Norwalk, CT: Business Communications Co., Inc., 2001. pp. 54-69